Available online at www.eccomasproceedia.org
Eccomas Proceedia COMPDYN (2023) 925-938

ECCOMAS
Proceedia

COMPDYN 2023
9th ECCOMAS Thematic Conference on
Computational Methods in Structural Dynamics and Earthquake Engineering
M. Papadrakakis, M. Fragiadakis (eds.)
Athens, Greece, 12-14 June 2023

1D HARMONIC RESPONSE OF INHOMOGENEOUS SOIL DEPOSITS WITH EXPONENTIALLY VARYING STIFFNESS: EXACT & APPROXIMATE SOLUTIONS

Haralambos Parashakis[1], Emmanouil Rovithis[2], and George Mylonakis[3,4]

[1] Hellenic Mediterranean University
Heraklion, Greece
e-mail: parashaki_m@hotmail.com

[2] Department of Civil Engineering, Democritus University of Thrace
Xanthi, Greece
erovithis@civil.duth.gr

[3] Department of Civil Infrastructure and Environmental Engineering, Khalifa University
UAE
george.mylonakis@ku.ac.ae

[4] Department of Civil Engineering, University of Bristol
Bristol, UK
g.mylonakis@bristol.ac.uk

Abstract

The harmonic response of an inhomogeneous soil layer with exponentially varying stiffness with depth is explored by using one-dimensional viscoelastic wave propagation theory. An exact solution of the Bessel type is derived from the governing equation, which allows for: (i) a novel interpretation of the attenuation patterns with depth for soil strains, displacements and stresses without a counterpart in other relevant solutions; (ii) identification of the parameters that control soil curvatures close to soil surface and at depth. New approximate solutions are also proposed for the fundamental natural frequency of the layer and the base-to-surface transfer function at high and low frequencies, which show a good agreement with the exact solution. A full-domain approximation is finally proposed as an alternative to the complex exact solution furnishing base-to-surface transfer function over the entire frequency range which can be used in practical applications. A numerical example is presented.

Keywords: Dynamic loads, Earthquakes, Seismic Effects, Soil Dynamics

ISSN:2623-3347
Peer-review under responsibility of the organizing committee of COMPDYN 2023.
doi: 10.7712/120123.10446.21336

1 INTRODUCTION

Available analytical solutions for the seismic response of continuously inhomogeneous media reveal the possibility of higher amounts of seismic energy reaching the ground surface over media with discontinuous variation in elastic properties with depth [1]. Problems involving continuous inhomogeneity have been treated for different velocity models ([1], [2], [3], [4], [5], [6], [7], [8], [9], [10], [11], [12], [13], [14]), without necessarily acknowledging the importance of continuous versus discontinuous variation in soil material properties with depth. The effect of soil inhomogeneity has been studied in multiple dimensions for different types of waves. Vrettos [15] tackled the problem of dispersive SH-surface waves propagating in an inhomogeneous half-space for both bounded and unbounded variations of shear modulus with depth. A collection of available solutions (not restricted to elastic waves) for wave propagation in inhomogeneous media is available in Manolis and Shaw ([16], [17], [18]) and Brekhovskikh and Bayer [19]. Seismic response of inhomogeneous media modeled using "equivalent" homogeneous counterparts i.e. defined by means of an average wave propagation velocity, has been explored against exact solutions ([11], [14], [20], [21], [22]). Also, simple analytical formulae have been proposed for the fundamental dynamic characteristics of inhomogeneous soils at resonance conditions by means of Rayleigh approximations ([12]) and asymptotic analysis ([14], [23]).

Despite the research in the subject for over half a century, nearly all analytical solutions for inhomogeneous media are limited to cases where stiffness and shear wave propagation velocity vary as a power of depth. In this paper, the seismic response of an inhomogeneous soil layer resting on a rigid base is investigated in the realm of one-dimensional viscoelastic wave propagation theory. An exponential function is adopted, which can describe both positive and negative velocity gradients. The latter may be relevant for cases of large confining stresses under building foundations, stiff over-consolidated surface crusts or ground improvement near the soil surface, which may result in soil stiffness decreasing with depth ([13], [24]). The problem is treated analytically leading to an exact solution, expressed in terms of Bessel functions, for the vibrational characteristics of the system, the base-to-surface transfer function and the variation of soil displacements, shear strains and curvatures with depth. The solution is compared against Rayleigh approximations for the fundamental frequency of the layer, by implementing different shape functions for the corresponding mode shapes. Asymptotic and approximate solutions are proposed for the asymptotic response in low and high frequencies, which are combined through a smooth transition function to provide a full-domain approximation. The model is validated against a numerical layer transfer-matrix (Haskell-Thomson) formulation for an actual soil profile.

2 PROBLEM STATEMENT

The problem considered in this work refers to a continuously inhomogeneous viscoelastic soil layer of thickness H, excited by vertically propagating seismic shear (SH) waves applied at its base (Figure 1).

Soil mass density, ρ, and hysteretic damping ratio, ξ, are assumed constant with depth, while shear wave propagation velocity follows the exponential variation

$$V(z) = V_0 \, e^{\,\alpha \, z/z_r} \tag{1}$$

where V_0 is the shear wave propagation velocity at ground surface, z_r is a reference depth, and α is a dimensionless inhomogeneity parameter. Rearranging Equation 1, parameter α can be defined as:

$$\alpha = ln(V_0/V_H)^{-1} \tag{2}$$

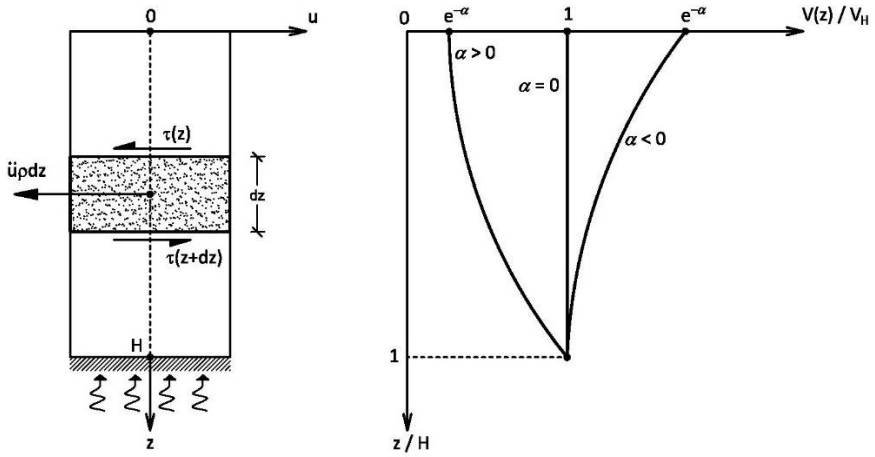

Figure 1: Inhomogeneous soil layer with exponentially varying shear wave velocity with depth over a rigid base.

where V_H (= $V_0 e^{\alpha}$) is the shear wave propagation velocity at the base ($z_r = H$). Evidently, positive and negative values of α correspond to stiffness increasing with depth ($V_0 < V_H$) and decreasing with depth ($V_0 > V_H$), respectively. For $\alpha = 0$, the model degenerates to a uniform velocity distribution ($V_0 = V_H$).

The input motion is specified at the base of the system in the form of a harmonic horizontal displacement, $u = u_0 \exp[i\,\omega\,t]$, $\omega = (2\pi f)$ being the cyclic excitation frequency, thereby generating shear waves propagating vertically up and down (upon reflection) in the profile.

3 ANALYTICAL DEVELOPMENTS

Under harmonic steady-state oscillations, one-dimensional shear waves in an inhomogeneous soil layer are described by the familiar ordinary differential equation ([1], [2]):

$$\frac{d}{dz}\left[G(z)\frac{du}{dz}\right] + \rho\omega^2 u = 0 \tag{3}$$

Upon introducing the displacement potential $Y(z)$ through the transformation $dY/dz = u(z)$ and integrating with respect to z, the governing equation in Equation 3 can be rewritten in the normal form:

$$\frac{d^2}{dz^2}Y + k^2(z)\,Y = 0 \tag{4}$$

where the term associated with the first derivative of the new dependent variable, dY/dz, has disappeared and the depth-varying shear modulus has escaped differentiation. In the latter equation,

$$k(z) = k_0\, e^{-\alpha\, z/z_r} \tag{5}$$

stands for the depth-varying wavenumber of the associated stress waves, where $k_0 = (\omega/V_0)$ is the value at ground surface. The solution to Equation 4 is

$$Y(z) = C_1\, J_0\left(\frac{k_0 z_r}{\alpha} e^{-\alpha\frac{z}{z_r}}\right) + C_2\, N_0\left(\frac{k_0 z_r}{\alpha} e^{-\alpha\frac{z}{z_r}}\right) \tag{6}$$

where $J_0(\,)$ and $N_0(\,)$ are the zero-order Bessel functions of the first and the second kind, respectively; C_1, C_2 are integration constants to be determined from the boundary conditions. Upon differentiating with depth, the general solution for displacements is obtained from Equa-

tion 6 as

$$u(z) = k_0\, e^{-\alpha\frac{z}{z_r}} \left[C_1\, J_1\left(\frac{k_0 z_r}{\alpha} e^{-\alpha\frac{z}{z_r}}\right) + C_2\, N_1\left(\frac{k_0 z_r}{\alpha} e^{-\alpha\frac{z}{z_r}}\right)\right] \tag{7}$$

where $J_1(\,)$ and $N_1(\,)$ denote the corresponding Bessel functions of the first order. The associated shear stresses can be derived by inspection, given that $\tau(z) = G(z)\ \gamma(z) = G(z)\ du/dz = G(z)\ d^2Y/dz^2 = -\rho\ \omega^2 Y$, to get

$$\tau(z) = -\rho\omega^2 \left[C_1\, J_0\left(\frac{k_0 z_r}{\alpha} e^{-\alpha\frac{z}{z_r}}\right) + C_2\, N_0\left(\frac{k_0 z_r}{\alpha} e^{-\alpha\frac{z}{z_r}}\right)\right] \tag{8}$$

The boundary condition of a traction-free surface, $\tau(0) = 0$, yields a proportionality relation between constants C_1 and C_2 [29]; the solution for displacements becomes

$$u(z) = C_1\, k_0\, e^{-\alpha\frac{z}{z_r}} \left[J_1\left(\frac{k_0 z_r}{\alpha} e^{-\alpha\frac{z}{z_r}}\right) N_0\left(\frac{k_0 z_r}{\alpha}\right) - J_0\left(\frac{k_0 z_r}{\alpha}\right) N_1\left(\frac{k_0 z_r}{\alpha} e^{-\alpha\frac{z}{z_r}}\right)\right] / N_0\left(\frac{k_0 z_r}{\alpha}\right) \tag{9}$$

From Equations 3 and 9, the corresponding solution for shear strain is

$$\gamma(z) = -\,C_1\, k_0^2\, e^{-2\alpha\frac{z}{z_r}} \left[J_0\left(\frac{k_0 z_r}{\alpha} e^{-\alpha\frac{z}{z_r}}\right) N_0\left(\frac{k_0 z_r}{\alpha}\right) - J_0\left(\frac{k_0 z_r}{\alpha}\right) N_0\left(\frac{k_0 z_r}{\alpha} e^{-\alpha\frac{z}{z_r}}\right)\right] / N_0\left(\frac{k_0 z_r}{\alpha}\right) \tag{10}$$

Finally, operating on Equation 3 one can easily establish the second derivative d^2u/dz^2, which expresses the curvature of soil with depth

$$(1/R) = -\,\{2\,[V'(z)/V(z)]\,\gamma + k^2(z)\,u\} \tag{11}$$

The above expression holds for general variations in shear wave propagation velocity with depth and it is not limited to a particular type of soil inhomogeneity. For the velocity model at hand (Equation 1) one obtains

$$(1/R) = -\left[(2\alpha/z_r)\,\gamma + k_o^2\, e^{-2\alpha\, z/z_r}\, u\right] \tag{12}$$

In light of these analytical developments, it is worthy of note that the multipliers exp $(-2\alpha\ z/z_r)$ and exp $(-\alpha\ z/z_r)$ appear, respectively, in the expressions for strains in Equation 10 and displacements in Equation 9, but not in the one for stresses (Equation 8). For the common case of positive a, this implies that strains and displacements attenuate with depth faster than stresses, while strains attenuate with depth faster than displacements. This is different from other basic problems in geo-mechanics, such as the Boussinesq point-load solution, where stresses attenuate with depth faster than displacements ([25], [26]). The slower attenuation of stresses relative to strains and displacements in the problem at hand can be interpreted in light of the direct dependence of stresses on dynamic equilibrium with the imposed inertial loads, which forces stresses to exhibit a more "statically determined" behavior than the other response functions. Also, for positive values of a, soil curvature $(1/R)$ attenuates rapidly with depth, as evident from the exponential multipliers $\exp(-2a\ z/z_r)$ and $\exp(-3a\ z/z_r)$ in the first and second term in the right-hand side of Equation 12. As the term associated with soil displacement attenuates faster than the one for strain, curvatures at depth tend to be governed by strains. On the other hand, shear strain at soil surface, $\gamma(0)$, is always zero, as shear stress is by definition zero, while the corresponding shear modulus, $G(0)$, is finite, while for $z = 0$, the displacement at soil surface is obtained as:

$$u(0) = C_1\left(\frac{2\alpha}{\pi z_r}\right) / N_0\left(\frac{k_0 z_r}{\alpha}\right) \tag{13}$$

3.1 Natural frequencies and mode shapes

Setting the reference depth $z_r = H$ and considering undamped free oscillations, the displacement at the base of the layer must be zero [$u(H) = 0$]. Enforcing this condition to Equation 9 yields the characteristic equation:

$$J_1\left(\frac{k_n H}{\alpha}e^{-\alpha}\right)N_0\left(\frac{k_n H}{\alpha}\right) - J_0\left(\frac{k_n H}{\alpha}\right)N_1\left(\frac{k_n H}{\alpha}e^{-\alpha}\right) = 0 \tag{14}$$

the solution to which provides the (infinite) eigenvalues of the layer. Given the transcendental nature of Equation 14, the eigenvalues need to be established numerically; these can be written in normalized form as

$$\frac{f_n}{f_{1H}} = \frac{2}{\pi}k_n H e^{-\alpha} \qquad n = 1, 2, 3,... \tag{15}$$

where k_n (= ω_n/V_0) is the eigen-wavenumber at the surface and f_{1H} (=$V_H/4H$) is the fundamental natural frequency of a homogeneous layer of the same thickness as the inhomogeneous one, and shear wave propagation velocity equal to the wave velocity at the base, V_H. Normalizing Equation 9 by $u(0)$ in Equation 13 and introducing the dimensionless depth $\eta = z/H$ yields the dimensionless mode shape

$$\Phi(\eta) = \frac{\pi}{2}\left(\frac{k_n H}{\alpha}e^{-\alpha\eta}\right)\left[J_1\left(\frac{k_n H}{\alpha}e^{-\alpha\eta}\right)N_0\left(\frac{k_n H}{\alpha}\right) - J_0\left(\frac{k_n H}{\alpha}\right)N_1\left(\frac{k_n H}{\alpha}e^{-\alpha\eta}\right)\right] \tag{16}$$

3.2 Steady state harmonic response

Taking the ratio of Equations 13 and 9 and setting $z = H$, the amplification function of the inhomogeneous soil layer is readily obtained as:

$$F(\omega) \equiv \frac{u(0)}{u(H)} = \frac{2}{\pi}\left\{\left(\frac{k_0 H}{\alpha}e^{-\alpha}\right)\left[J_1\left(\frac{k_0 H}{\alpha}e^{-\alpha}\right)N_0\left(\frac{k_0 H}{\alpha}\right) - J_0\left(\frac{k_0 H}{\alpha}\right)N_1\left(\frac{k_0 H}{\alpha}e^{-\alpha}\right)\right]\right\}^{-1} \tag{17}$$

where k_0 is now a continuous function of excitation frequency ω. Note that soil material damping, ξ, can be readily accounted for in the above expression by replacing the real wavenumber with its complex counterpart $k_0^* = k_0/\sqrt{1 + 2i\xi}$ ([27], [28]).

The analytical base-to-surface transfer function in Equation 17 is plotted in Figure 2a and 2b for $V_0 \leq V_H$ ($a > 0$) and $V_0 \geq V_H$ ($a < 0$), respectively, with the abscissa normalized by the exact fundamental frequency of the inhomogeneous layer, f_1, obtained numerically from Equation 14. All the plots in Figure 2 refer to constant hysteretic damping ratio of the soil at $\xi = 0.05$. Evidently, the spacing between successive resonant peaks for $V_0 \leq V_H$ gets "compressed" (i.e. the ratios f_n/f_1 become smaller than in a homogeneous layer) with increasing inhomogeneity. Also, the amplification amplitude at a particular resonant peak increases relative to that of a more homogeneous layer. The opposite is true for the case when $V_0 \geq V_H$; the natural frequencies tend to get "stretched" relative to f_1 and their amplitudes decrease relative to those of a more homogeneous layer. In all cases, the amplitudes of successive resonance peaks decrease with frequency.

4 RAYLEIGH APPROACH

Considering a unitary dimensionless shape function, $\psi(z)$, representing the fundamental mode shape of the inhomogeneous layer, $\Phi_1(z)$, constant mass density and the normalized shear wave propagation velocity $\bar{V}_s(\eta) = V_s(\eta)/V_H = e^{+\alpha(\eta-1)}$, the familiar Rayleigh quotient ([9], [12]) can be re-written in normalized form as ([29]):

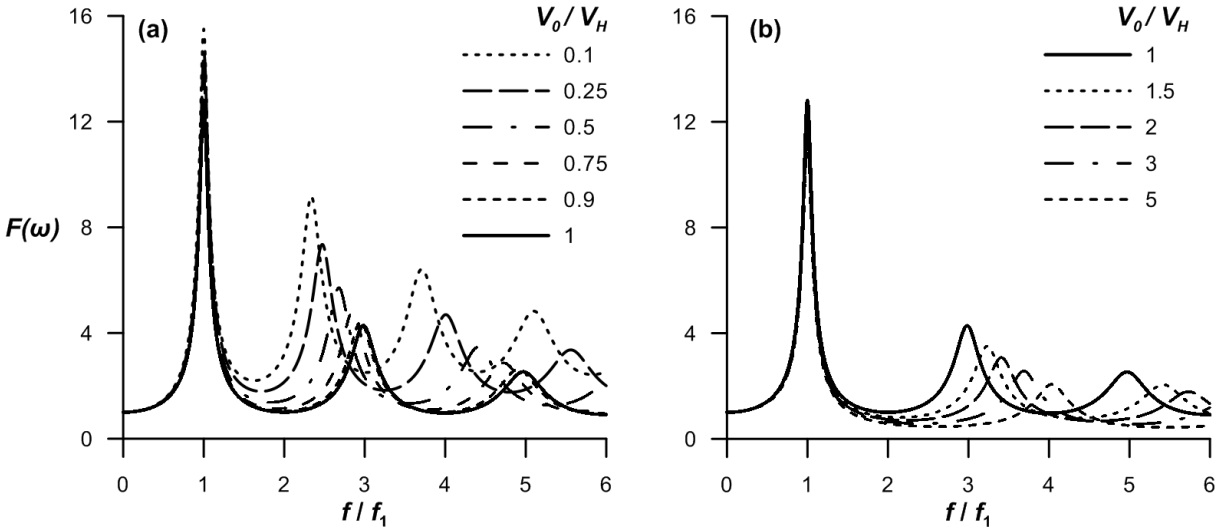

Figure 2: Effect of V_0/V_H ratio on base-to-surface transfer function of the inhomogeneous layer for (a) $V_0 \leq V_H$, and (b) $V_0 \geq V_H$. In all plots, $\xi = 0.05$.

$$f_1/f_{1H} = (2/\pi)\left[\int_0^1 \bar{V}_s^2(\eta)(\psi'(\eta))^2\, d\eta \,/\, \int_0^1 \psi^2(\eta)\, d\eta\right]^{1/2} \tag{18}$$

Shape function	$\boldsymbol{\psi(\eta)}$	***Fundamental Frequency*** $(\boldsymbol{f_1/f_{1H}})$
Linear	$1-\eta$	$(2/\pi)[(3/2\alpha)(1-e^{-2\alpha})]^{1/2}$
Parabolic	$1-\eta^2$	$(2/\pi)[(15/8\alpha^3)(1+2\alpha^2-2\alpha-e^{-2\alpha})]^{1/2}$
Sinusoidal	$cos\left(\frac{\pi}{2}\eta\right)$	$\left[(\pi^2(1-e^{-2\alpha})+8\alpha^2)/\left(2\alpha(4\alpha^2+\pi^2)\right)\right]^{1/2}$
Compatible	$[(2\alpha+1)e^{-2\alpha}-(2\,\alpha\,\eta+1)e^{-2\alpha\eta}]$ $/[(2\,\alpha+1)e^{-2\alpha}-1]$	$\frac{2}{\pi}[32\alpha^2(e^{2\alpha}-2\alpha^2-2\alpha-1)/s]^{1/2}$ $s = 32\alpha^3+56\alpha^2+44\alpha-16\,(2\alpha+1)\,e^{2\alpha}$ $+5\,e^{4\alpha}+11$

Table 1: Rayleigh expressions for the fundamental natural frequency based on different shape functions.

Following Mylonakis et al. [12], four shape functions are examined (Table 1): linear, parabolic, sinusoidal and "compatible". The last function is obtained by imposing a distributed horizontal static load, proportional to soil mass along the height of the column ([29]). The Rayleigh solutions are compared against the numerically - evaluated exact solution in Figure 3 for different values of the inhomogeneity factor α.

5 ASYMPTOTIC AND APPROXIMATE SOLUTIONS

5.1 Asymptotic behavior at high frequencies

Employing pertinent asymptotic expressions of the Bessel functions for large arguments, it can be shown that the amplification function in Equation 17 simplifies to

$$F_h(\omega) \sim e^{\alpha/2}/cos[k_0 H(1-e^{-\alpha})/\alpha] \tag{19}$$

The above expression can be used to provide reasonable approximations of the higher

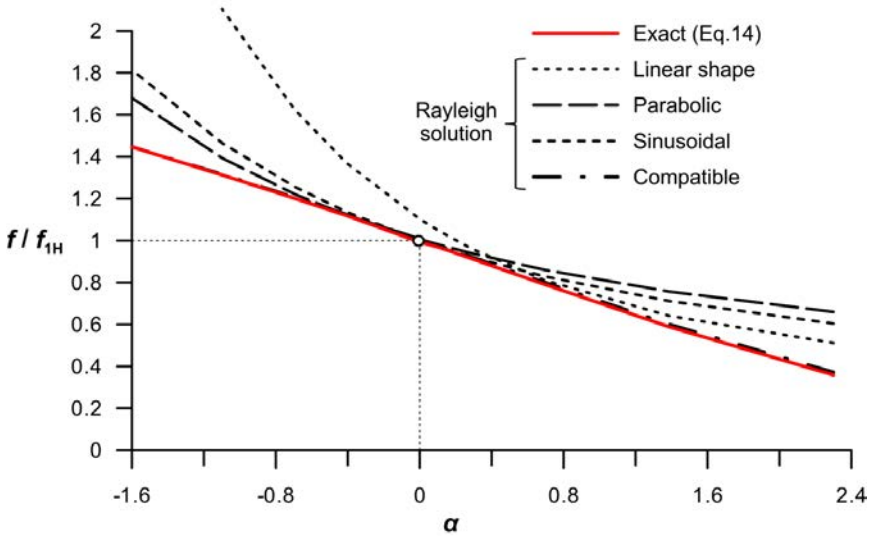

Figure 3: Normalized fundamental frequency of the inhomogeneous layer as function of the inhomogeneity parameter α. Comparison of the exact solution with approximate Rayleigh solutions obtained using Equation 18.

resonant frequencies of the inhomogeneous stratum by means of the characteristic equations

$$cos[k_0 H(1 - e^{-\alpha})/a] = 0\ ,\ cos[k_H H(e^{\alpha} - 1)/a] = 0 \tag{20}$$

the solution to which is

$$(k_H H)_k (e^{\alpha} - 1)/a = (2k - 1)\,\pi/2, \qquad k = 1, 2, 3, \ldots \tag{21}$$

where k_H (= ω / V_H) is the wavenumber at the base of the layer.

In light of Equation 21, the following equivalent shear wave propagation velocity in the high-frequency range, $V_{eq,h}$, can be defined:

$$V_{eq.h} = V_H\, \alpha\ /\ (e^{\alpha} - 1) \tag{22}$$

The asymptotic solution in Equation 19 is compared to the exact one (Equation 17) in Figure 4 for different V_0/V_H ratios. In the abscissa, excitation frequency is normalized by the exact fundamental frequency, f_1, of the inhomogeneous layer. The agreement between the two solutions beyond first resonance highlights the validity of the asymptotic solution at high frequencies. Evidently, Equation 19 allows a reasonable approximation of the high-frequency response of the inhomogeneous layer for frequencies beyond approximately 1 to 2 times the fundamental natural frequency f_1. Beyond second resonance (i.e. 2 to 4 times f_1), the agreement between the results from Equation 19 and the exact solution is nearly perfect.

5.2 Strain-velocity and curvature-acceleration relations

Using the pertinent asymptotic expansions of the relevant Bessel functions for large arguments, it is straightforward to show that at high frequencies, strain amplitude at depth is related to particle velocity at the surface through the ratio

$$\gamma(z) \cong -\dot{u}(0)/V(z) \tag{23}$$

which is an extension of the familiar relation for homogeneous soil ([28]). Likewise, operating on Equation 12, curvature at shallow depths can be related to particle acceleration at the surface through

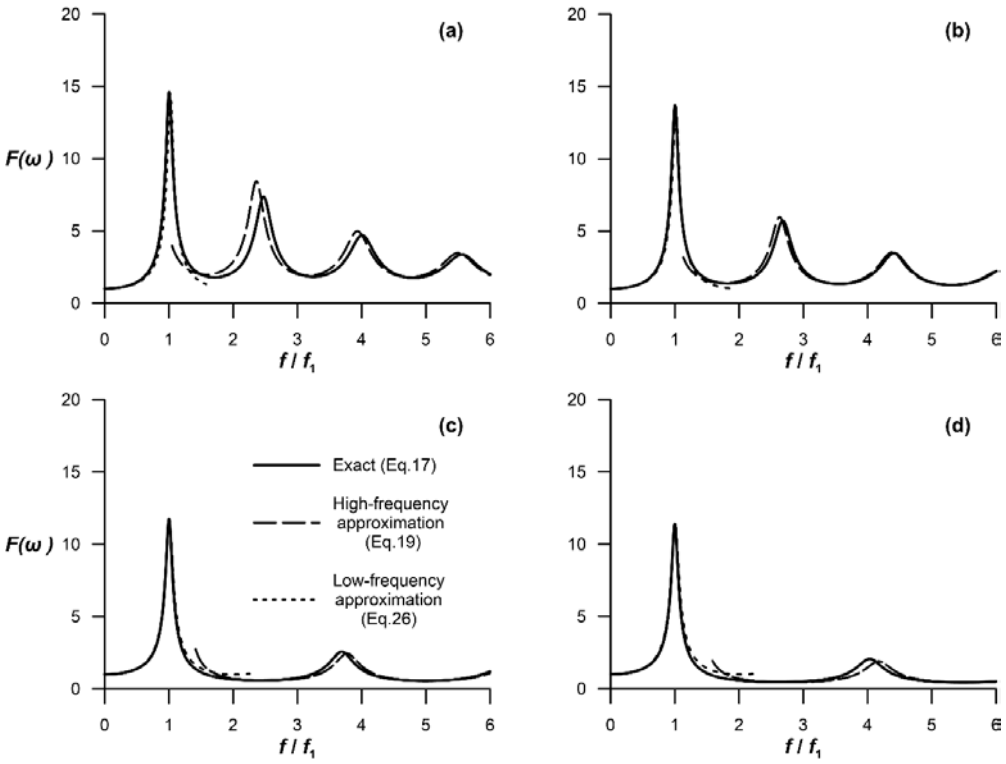

Figure 4: Comparison of the base-to-surface amplification function between the exact solution (Equation 17), the high-frequency approximation (Equation 19) and the low-frequency approximation (Equation 26) for V_0/V_H ratio at (a) 0.25, (b) 0.5, (c) 3 and (d) 5; $\xi = 0.05$, $\xi_{eq.l}$ from Equation 28

$$1/R(z) \cong \ddot{u}(0)/V^2(z) \tag{24}$$

Remarkably, the last two equations are related through the expression *1/R(z) = k(z)γ(z)* which, again, is a generalized form of available solutions for homogeneous soil ([30], [31]). On the other hand, curvature at depth is related to corresponding shear strain via the equation

$$1/R(z) \cong -2\,[V'(z)/V(z)]\gamma(z) = -2\,\gamma(z)\,a/H \tag{25}$$

which indicates that the absolute thickness of the layer has an influence on curvatures deep beneath the soil surface. The last equation has no counterpart in available solutions for homogeneous soil.

5.3 Low-frequency approximation

The following approximate relation is proposed for the amplification function (Equation 17) at low frequencies

$$F_l(\omega) \cong 1/\cos\left(k_{eq.l}\,H\right) \tag{26}$$

which satisfies the limit condition $F(0) = 1$. In the above equation, ($k_{eq.l}$ H) is a dimensionless wavenumber that reproduces the first resonance. The corresponding wave velocity can be determined using the Rayleigh approach for the compatible shape function (Table 1) by means of the equation

$$V_{eq,l} = 4f_{1,com}H \tag{27}$$

where $f_{1,com}$ is the fundamental frequency of the layer. Given that the corresponding resonant

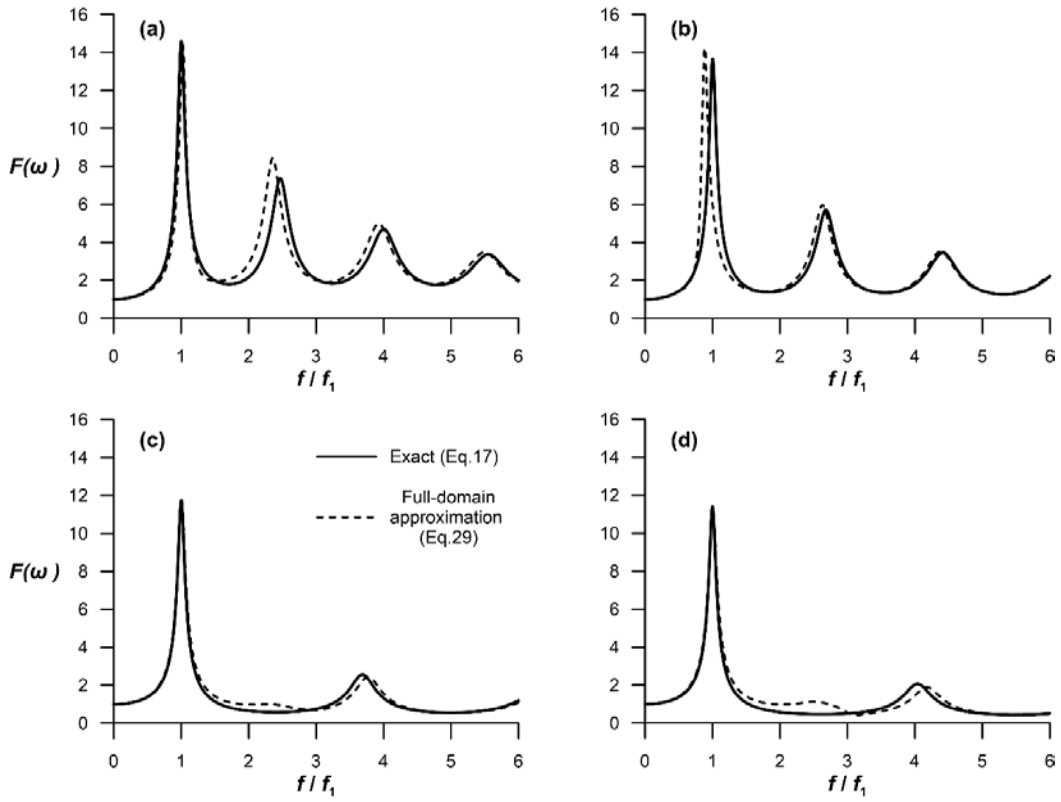

Figure 5: Comparison of the base-to-surface amplification function between the exact solution (Equation 17) and the full-domain approximation in Equation 29 for V_0/V_H ratio at (a) 0.25, (b) 0.5, (c) 3 and (d) 5; $\xi = 0.05$.

peak in an inhomogeneous layer has a different amplitude than in a homogeneous one, the following empirical correction, back-calculated from the numerical data, is proposed for the equivalent damping ratio

$$\xi_{eq.l} \cong (1 - 0.08\,\alpha)\,\xi \tag{28}$$

where ξ is the actual soil material damping. No such correction is needed for higher resonances. The approximate solution in Equation 28 is plotted in Figure 4 for comparison. The agreement with the exact solution cannot be overstated. It is stressed that this low-frequency approximation is valid near first resonance. If Equations 26-28 are implemented for frequencies past approximately 2 times the fundamental natural frequency f_1, they may induce large errors depending on the characteristics of the layer.

5.4 Full-domain approximation

Based on the foregoing, a full-domain approximation is possible according to the connection formula:

$$F(\omega) \cong F_l(\omega)\,q(\omega) + F_h(\omega)\,[1 - q(\omega)] \tag{29}$$

where $q(\omega)$ is a smooth transition function adopted based on ([33])

$$q(\omega) \cong 1/\{1 + [k_0 H\,/(\chi_1\, e^{\chi_2 \alpha}\alpha)]^{\chi_3}\} \tag{30}$$

The vector of the fitted parameters (χ_1, χ_2, χ_3) was established numerically at (2.5, 0.25, 20) for $V_0/V_H < 1$ and (7.5, 1.4, 20) for $V_0/V_H > 1$, respectively. The full-domain approximation is successfully compared against the exact solution in Figure 5.

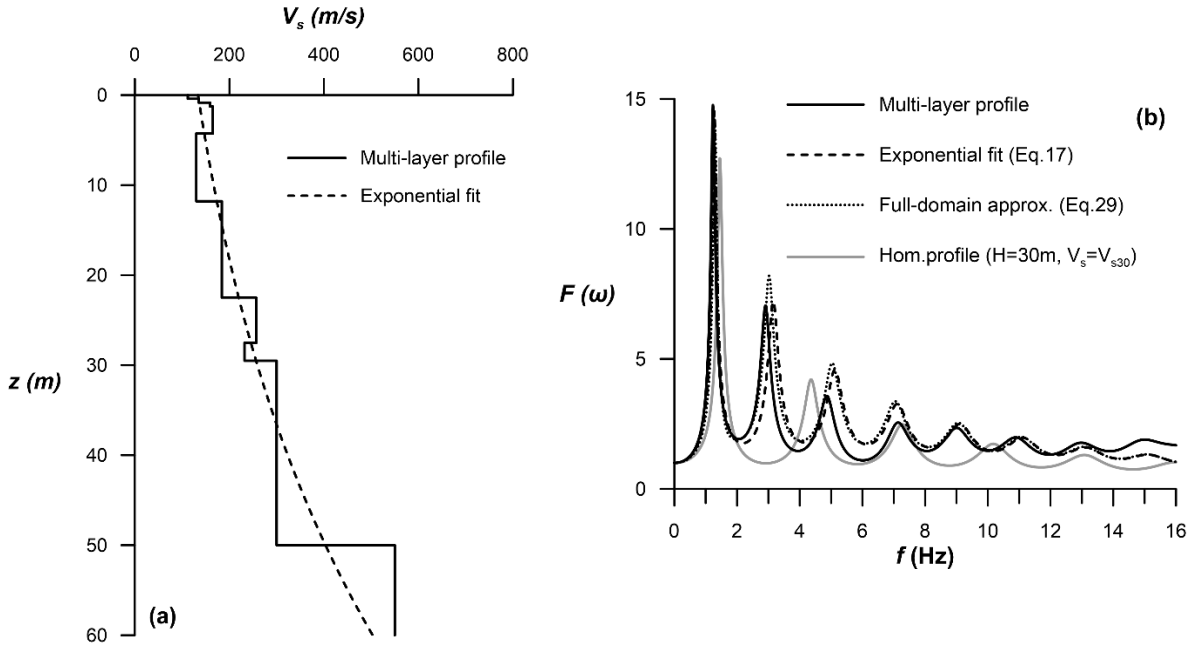

Figure 6. (a) Discontinuous V_s profile employed as representative of San Francisco Bay area ([32]). (b) Comparison of amplification functions using the exact solution for the actual (layered) soil profile, the exact solution in Equation 17, the full-domain approximation in Equation 29 for the exponential model, and a solution for a homogeneous layer based on a V_{s30} approximation:

6 NUMERICAL EXAMPLE

An actual profile with discontinuous variation in shear wave propagation velocity with depth was employed to assess the proposed solutions against a numerical simulation of soil response using a series of a piece-wise homogeneous layers, implemented through the classical Haskell-Thompson algorithm, which involves a sequence of transfer-matrix multiplications ([27], [34]) To this end, a real multi-layer soil deposit typical of the San Francisco Bay Area ([32]), resting on bedrock at a depth of approximately 60 m, was selected. The shear wave propagation velocity profile is plotted in Figure 6a up to the elevation of - 60 m, following the above reference. Soil mass density and hysteretic damping ratio were assumed constant with depth, equal to 2 Mg/m^3 and 5% respectively. The exponential function velocity model was established by employing a least-squares fit. In this manner, the vector (V_0, V_0/V_H) was established at approximately (134 m/s, 0.265) for the soil profile under consideration. Accordingly, the dimensionless inhomogeneity parameter α is equal to 1.326 and the exponential velocity profile is given by (Figure 6a):

$$V(z) = 134\, e^{+0.0221\, z} \qquad [\text{in } m/s] \tag{31}$$

The exact base-to-surface transfer function computed for the above exponential model by means of Equation 17 and the prediction of the full-domain approximation (Equation 29) are compared to the reference numerical Haskell-Thompson solution in Figure 6b. The close agreement of the analytical solutions with the numerical one, which is evident, especially in the low-to-intermediate frequency range up to 5 Hz, highlights the applicability of these expressions when the velocity profile of a real soil deposit can be approximated by an exponential function. A code-based approximation, referring to the response of a 30 m thick homogeneous layer with shear wave velocity equal to V_{s30}, as defined in EC8, is also shown in Figure 6b. The large discrepancies observed between the V_{s30} approximation and the more rigorous solutions beyond

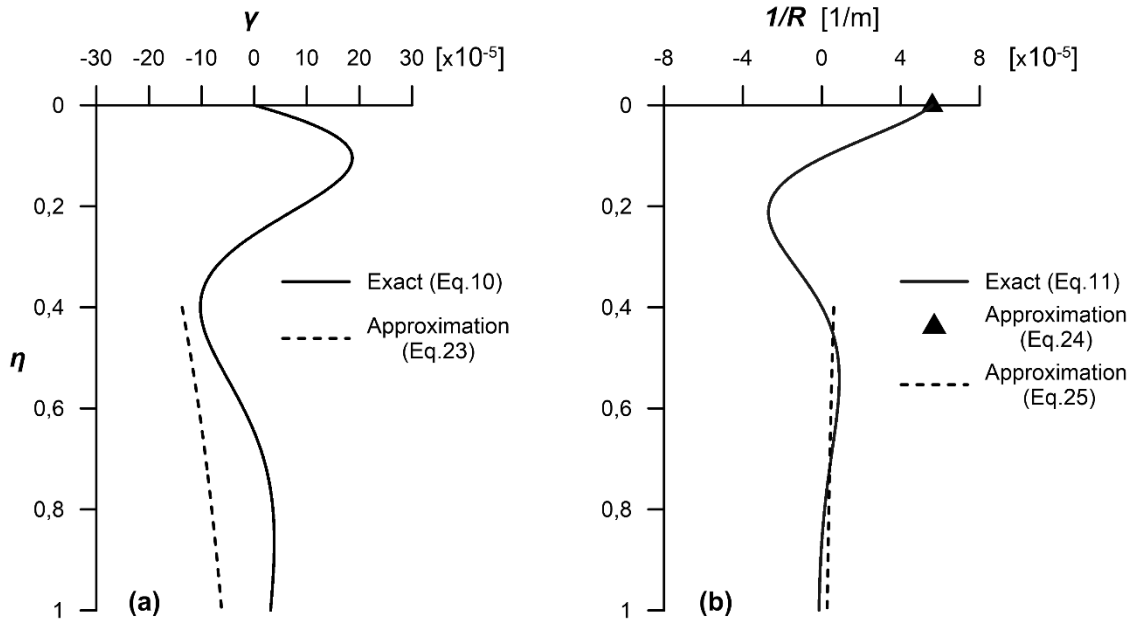

Figure 7. Comparison of shear strains (a) and curvatures (b) with depth, between the exact solution and the approximate solutions in Equations 23, 24 and 25; $\ddot{u}(0) = 1$ m/s^2, $f = f_3 = 5.13$ Hz, $\xi = 0.05$.

the first resonance indicates the inability of such a simplified approach to capture the actual response of inhomogeneous soil and should thus be employed with caution, especially for deep soil deposits excited by high-frequency motions.

The shear strain and curvature profiles with depth are further explored in Figure 7, in light of Equations 23-25. The approximate relations are compared to the exact solution for a unit ground surface acceleration at a frequency $f = 5.13$ Hz corresponding to third resonance. It is observed that Equation 23 (plotted for $\eta = z/H > 0.4$) provides a somewhat conservative prediction of shear strain at depth. With reference to curvature, the general solution in Equation 11 duly reduces to Equation 24 at $z = 0$ where the shear strain at soil surface, $\gamma(0)$, is zero. Thus, Equation 24 is applicable regardless of the type of inhomogeneity. This property is particularly important when the soil interacts with embedded structural elements like piles or diaphragm walls, so that strains and curvatures are "transferred" from the soil to the structural elements. Relevant discussions on strain and curvature transmissibility pertaining to piles are provided in Di Laora et al [30], Mylonakis [35], Anoyatis et al [36] and in a recent review article by Di Laora and Rovithis [31]. However, this topic lies beyond the scope of the paper. Further, Equation 25 provides a good approximation of curvature at depth, which reflects the dominant contribution of strain in this case.

7 CONCLUSIONS

An analytical solution was derived for the dynamic response of a soil layer with stiffness varying exponentially with depth. The main conclusions drawn from the study are:

- For the velocity model at hand, strains and displacements attenuate with depth much faster than stresses, while strains attenuate with depth faster than displacements. The slower attenuation of stresses with depth relative to displacements and strains could be interpreted in light of the direct dependence of stresses on dynamic equilibrium that forces them to exhibit a more "statically determined" behavior than the other response functions.
- For positive values of the inhomogeneity parameter a, soil curvature ($1/R$) attenuates fast with depth, as evident by the exponential multipliers in the first and second term in the right-

hand side of Equation 12. As the associated displacement term attenuates with depth faster than that of strain, curvature at depth tends to be governed by the strain component.

- With reference to the base-to-surface transfer function in Equation 17, for $V_0 \leq V_H$ ($a > 0$), the frequencies of resonant peaks tend to get "compressed" (i.e. the ratios f_n/f_1 become smaller than in the homogeneous layer) with increasing inhomogeneity. Also, the amplitude of a resonant peak increases relative to the same peak in a more homogeneous layer. The opposite is true for $V_0 \leq V_H$: the frequencies of the resonant peaks tend to get "stretched" relative to the f_1 with increasing inhomogeneity. Also, their amplitudes tend to decrease relative to that of a less inhomogeneous layer. In all cases, the peak amplitudes at successive resonance peaks are a decreasing function of frequency.
- The compatible shape function in Table 1 provides excellent predictions of the fundamental natural frequency of the soil layer using the Rayleigh quotient (Equation 18). In the special case where $a \rightarrow 0$, the compatible shape function collapses into the parabolic one in Table 1.
- The asymptotic and approximate solutions in Equations 19 and 26 provide good approximations of the high- and low-frequency behavior of the amplification function. To match the response amplitude at first resonance (which is higher than in a homogenous layer for $V_0 < V_H$ and lower for $V_0 > V_H$), an empirical adjustment in damping was proposed in Equation 28.
- Equation 23 provides realistic yet somewhat conservative predictions of strain at depth and/or high frequencies. On the other hand, Equation 24 provides exact values of curvature at ground surface. This is true regardless of the specific velocity profile, provided that shear strain at the surface, $\gamma(0)$, is zero. This property has important implications in soil-structure interaction e.g. in kinematic bending of piles. Equation 25 provides a good approximation of curvature at depth, which reflects the dominant contribution of soil strain in this case.
- The full-domain approximation proposed in Equation 29 and 30 provides good predictions of the exact solution in Equation 17 and allows application of the exponential velocity model in applications, both in frequency and time domains.

As a final remark, the solution at hand can be readily extended to encompass an arbitrary number of inhomogeneous layers, or a combination of stacked homogeneous and inhomogeneous layers by means of multiplications of transfer matrices ([29])

REFERENCES

[1] I. Towhata, Seismic wave propagation in elastic soil with continuous variation of shear modulus in the vertical direction. *Soils and Foundations,* 36(1): 61-72, 1996.

[2] W.M. Ewing, W.S. Jardetzky, *Elastic waves in layered media*. McGraw-Hill, NY, US, 1957.

[3] N. Ambraseys A note on the response of an elastic overburden of varying rigidity to an arbitrary ground motion. *Bulletin of the Seismological Society of America,* 49(3): 211-220, 1959.

[4] K. Toki and S. Cherry, Inference of subsurface accelerations and strain from accelerograms recorded at ground surface. In: *Proceedings of the 4th European Symposium on Earthquake Engineering*. European Academy on Earthquake Engineering, London, UK, 1972.

[5] H. Schreyer, One-dimensional elastic waves in inhomogeneous media. *Journal of the Engineering Mechanics Division ASCE*, 103(5): 979-990, 1977.

[6] G. Gazetas, Vibrational characteristics of soil deposits with variable wave velocity. International. *Journal for Numerical and Analytical Methods in Geomechanics,* 6: 1-20, 1982.

[7] P. Dakoulas, G. Gazetas, A class of inhomogeneous shear modes for seismic response of dams and embankments. *Soil Dynamics and Earthquake Engineering*, 4(4):166-82, 1985.

[8] K. Aki, Local site effects on weak and strong ground motion. *Tectonophysics* 218(1-3): 93-111, 1993.

[9] J.F. Semblat and A. Pecker, *Waves and Vibrations in Soils: Earthquakes, Traffic, Shocks, Construction Works*. IUSS Press, Pavia, Italy, 2009.

[10] Ch. Paraschakis, E. Rovithis and G. Mylonakis, 1D seismic response of layered inhomogeneous soil: A closed form solution. In *Proceedings of the 9th International Congress on Mechanics. Hellenic Society for Theoretical & Applied Mechanics (HSTAM)*, Limassol, Cyprus, pp. 639-647, 2010.

[11] E. Rovithis, Ch. Paraschakis, G. Mylonakis, 1D harmonic response of layered inhomogeneous soil: Analytical investigation. *Soil Dynamics and Earthquake Engineering*, 31(7): 879–890, 2011.

[12] G. Mylonakis, E. Rovithis and Ch. Paraschakis, 1D harmonic response of layered inhomogeneous soil: exact and approximate analytical solutions. In *Computational Methods in Earthquake Engineering* (Papadrakakis M, Fragiadakis M, and Plevris V (eds)). Springer, Vol. 2, pp. 1–32, 2013.

[13] Ch. Vrettos, Dynamic response of soils deposits to vertical SH waves for different rigidity depth-gradients. *Soil Dynamics and Earthquake Engineering* 47: 41-50, 2013.

[14] J. Garcia-Suarez, Application of path-independent integrals to soil-structure interaction. *PhD Dissertation*, California Institute of Technology, USA, 2020.

[15] Ch. Vrettos, Dispersive SH-surface waves in soil deposits of variable shear modulus. *Soil Dynamics and Earthquake Engineering* 9(5): 255-264, 1990.

[16] G.D. Manolis GD and R.P. Shaw, Harmonic elastic waves in continuously heterogeneous random layers. *Engineering Analysis with Boundary Elements* 19(3): 181-198, 1997.

[17] G.D. Manolis GD and R.P. Shaw, Numerical simulation of transient waves in a heterogeneous soil layer. *Computational Mechanics* 23: 75-86, 1999.

[18] G.D. Manolis GD and R.P. Shaw, Fundamental solutions for variable density two-dimensional elastodynamic problems. *Engineering Analysis with Boundary Elements* 24(10): 739-750, 2000.

[19] L.M. Brekhovskikh and R. Bayer R, *Waves in Layered Media*. Academic Press, New York, 1976.

[20] I.M. Idriss and H.B. Seed, Response of horizontal soil layers during earthquakes, *Research Report, Soil Mechanics and Bituminous Materials Laboratory*, University of California, Berkeley, 1967.

[21] R. Dobry, R. Whitman and J.M. Roesset, Soil properties and the one-dimensional theory of earthquake amplification. M.I.T., Department of Civil Engineering, USA, Report R71-18, 1971.

[22] J.X. Zhao, Modal analysis of soft-soil sites including radiation damping. *Earthquake Engineering and Structural Dynamics*, 26(1): 93-113, 1997.

[23] J. Garcia-Suarez, E. Esmaeilzadeh and D. Asimaki, Seismic harmonic response of inhomogeneous soil: scaling analysis, *Géotechnique*, https://doi.org/10.1680/jgeot.19.P.042, 2020.

[24] R. Dobry, I. Oweis and A. Urzua, Simplified procedures for estimating the fundamental period of a soil profile. *Bulletin of the Seismological Society of America,* 66(4):1293-1321, 1976.

[25] H.G. Poulos and E. H. Davis, *Elastic solution for soil and rock mechanics*. New York: John Wiley & Sons, 1974.

[26] R.O. Davis and Selvadurai A. P. S., *Elasticity and geomechanics*. Cambridge, UK: Cambridge University Press, 1996.

[27] J.M. Roesset, Soil amplification of earthquakes, In *Numerical methods in geotechnical engineering*, edited by C. H. Desai, 639–682. New York: McGraw-Hill, 1977.

[28] L.S. Kramer, *Geotechnical earthquake engineering*, Englewood, Cliff, NJ: Prentice Hall, 1996.

[29] E. Rovithis and G. Mylonakis, Seismic response of inhomogeneous soil deposits with exponentially varying stiffness, *Journal of Geotechnical and Geoenviromental Engineering*, 148(11), 0402209, 2022.

[30] R. Di Laora, G. Mylonakis, and A. Mandolini, Size limitations for piles in seismic regions." *Earthquake Spectra* 33 (2): 729–756, 2017.

[31] R. Di Laora, and E. Rovithis, Design of piles under seismic loading, In *Analysis of pile foundations subject to static and dynamic loading*, 269–300. Boca Raton, FL: CRC Press, 2021.

[32] G. Gazetas, and R. Dobry, Horizontal response of piles in layered soils, *Journal of Geotechnical and Geoenvironmental Engineering*, 110 (1): 20–40, 1984.

[33] M. Abramowitz and Stegun I. *Handbook of mathematical functions with formulas, graphs, and mathematical tables*. New York: Dover, 1965.

[34] W.P. Thompson, Transmission of elastic waves through a stratified soil strata. *Journal of Applied Physics*, 21:89–93, 1950.

[35] G. Mylonakis, Simplified Model for Seismic Pile Bending at Soil Layer Interfaces, *Soils & Foundations*, 41(4): 47-58, 2001.

[36] G. Anoyatis, R. Di Laora, A. Mandolini, and G. Mylonakis, Kinematic response of single piles for different boundary conditions: Analytical solutions and normalization scheme. *Soil Dynamics and Earthquake Engineering* **44**, 183-195, 2013.